

International Journal of Modern Physics A  
 © World Scientific Publishing Company

## THERMODYNAMICS IN NJL-LIKE MODELS

FRIESEN A.V

*Bogoliubov Laboratory of Theoretical Physics, Joint Institute for Nuclear Research, 141980  
 Dubna, Russia  
 aufriesen@theor.jinr.ru*

KALINOVSKY Yu.L.

*Laboratory of Information Technologies, Joint Institute for Nuclear Research, 141980 Dubna,  
 Russia  
 Higher Mathematics Department, University "Dubna", Dubna, Russia  
 kalinov@jinr.ru*

TONEEV V.D.

*Bogoliubov Laboratory of Theoretical Physics, Joint Institute for Nuclear Research, 141980  
 Dubna, Russia  
 toneev@theor.jinr.ru*

Received Day Month Year

Revised Day Month Year

Thermodynamic behavior of conventional Nambu-Jona-Lasinio and Polyakov-loop-extended Nambu-Jona-Lasinio models is compared. A particular attention is paid to the phase diagram in the  $(T - \mu)$  plane.

*Keywords:* NJL; PNIL; phase diagram.

PACS numbers: 11.30.Rd, 12.20.Ds, 14.40.Be

### 1. Introduction

Models of the Nambu-Jona-Lasinio (NJL) type<sup>1,2</sup> have a long history and have been extensively used to describe dynamics of lightest hadrons and thermodynamic properties of excited matter (see review articles<sup>3-7</sup>). In the “classical” versions such schematic models incorporate the chiral symmetry of two-flavor QCD and its spontaneous breakdown at the temperature below critical one,  $T < T_c$ , and offer a simple and practical illustration to the basic mechanisms that drive the spontaneous breaking of chiral symmetry, a key feature of QCD in its low-temperature low-density phase. However, in spite of the widespread use, the NJL models suffer a major shortcoming that the reduction to global color symmetry prevents quark confinement.

In the PNJL model<sup>8-12</sup>, the Polyakov-loop-extended NJL model, the quarks are coupled simultaneously to the chiral condensate, to be an order parameter of the

chiral symmetry breaking, and to a homogeneous gauge field representing Polyakov loop dynamics, which serves as an order parameter for the transition from low-temperature, symmetric, confined phase to the high-temperature, deconfined phase. The model has proven to be successful in reproducing lattice data on QCD thermodynamics<sup>10</sup>

In this paper we are confront general properties of  $\pi$  and  $\sigma$  mesons as well as thermodynamics at finite temperature  $T$  and baryon chemical potential  $\mu$  calculated within the two-flavor NJL model with those in the PNJL one.

### 1.1. Nambu-Jona-Lasinio model

To describe the coupling between quarks and the chiral condensate in the scalar-pseudoscalar sectors, the two-flavor NJL model<sup>1,6,13,14</sup> is used with the following Lagrangian density:

$$\mathcal{L}_{\text{NJL}} = \bar{q} (i\partial - \hat{m}_0) q + G \left[ (\bar{q}q)^2 + (\bar{q}i\gamma_5\vec{\tau}q)^2 \right]. \quad (1)$$

where  $G[\text{GeV}^{-2}]$  is the coupling constant,  $\vec{\tau}$  is the Pauli matrix in the flavor space,  $\bar{q}$  and  $q$  are the quark fields (color and flavor indices are suppressed),  $\hat{m}_0$  is the diagonal matrix of the current quarks mass,  $\hat{m}_0 = \text{diag}(m_u^0, m_d^0)$ ,  $m_u^0 = m_d^0 = m_0$ .

The grand potential can be emerged from this Lagrangian. The thermodynamic potential associated with the mean-field approximation has the form<sup>13</sup>

$$\Omega_{\text{NJL}} = G\langle\bar{q}q\rangle^2 + \Omega_q, \quad (2)$$

with

$$\Omega_q = -2N_c N_f \int \frac{d^3p}{(2\pi)^3} E_p - 2N_c N_f T \int \frac{d^3p}{(2\pi)^3} [\ln N^+(E_p) + \ln N^-(E_p)] \quad (3)$$

where  $N^+(E_p) = 1 + e^{-\beta(E_p - \mu)}$  and  $N^-(E_p) = 1 + e^{-\beta(E_p + \mu)}$  with  $E_p = \sqrt{\mathbf{p}^2 + m^2}$  and the inverse temperature  $\beta = 1/T$ .

### 1.2. Nambu-Jona-Lasinio model with Polyakov-loop

The deconfinement in a pure  $SU(N_c)$  gauge theory can be simulated by introducing an effective potential for a complex Polyakov loop field. The PNJL Lagrangian<sup>10,15–24</sup> is

$$\mathcal{L}_{\text{PNJL}} = \bar{q} (i\gamma_\mu D^\mu - \hat{m}_0) q + G \left[ (\bar{q}q)^2 + (\bar{q}i\gamma_5\vec{\tau}q)^2 \right] - \mathcal{U}(\Phi[A], \bar{\Phi}[A]; T). \quad (4)$$

Here notation is the same as in Eq. (1).

Quark fields are related with the gauge field  $A^\mu$  through the covariant derivative  $D^\mu = \partial^\mu - iA^\mu$ . The gauge field is  $A^\mu = \delta_0^\mu A^0 = -i\delta_4^\mu A_4$  (the Polyakov calibration). The field  $\Phi$  is determined by tracing of the Polyakov loop  $L(\vec{x})$ <sup>10</sup>:

$$\Phi[A] = \frac{1}{N_c} \text{Tr}_c L(\vec{x}), \text{ where } L(\vec{x}) = \mathcal{P} \exp \left[ i \int_0^\beta d\tau A_4(\vec{x}, \tau) \right].$$

The gauge sector of the Lagrangian density (4) is described by an effective potential  $\mathcal{U}(\Phi[A], \bar{\Phi}[A]; T)$  fitted to lattice QCD simulation results in a pure  $SU(3)$  gauge theory at finite  $T$ <sup>10,15</sup>

$$\frac{\mathcal{U}(\Phi, \bar{\Phi}; T)}{T^4} = -\frac{b_2(T)}{2} \bar{\Phi}\Phi - \frac{b_3}{6} (\Phi^3 + \bar{\Phi}^3) + \frac{b_4}{4} (\bar{\Phi}\Phi)^2 \quad (5)$$

$$b_2(T) = a_0 + a_1 \left(\frac{T_0}{T}\right) + a_2 \left(\frac{T_0}{T}\right)^2 + a_3 \left(\frac{T_0}{T}\right)^3. \quad (6)$$

Parameters of the effective potential (5) and (6) defined from fitting to the lattice results are summarized in Table 1.

Table 1. The effective potential parameters of  $\mathcal{U}[A]$ .

$a_0$	$a_1$	$a_2$	$a_3$	$b_3$	$b_4$
6.75	-1.95	2.625	-7.44	0.75	7.5

The parameter  $T_0$  is in the range from 190 MeV to 270 MeV. In the present work we use  $T_0 = 270$  MeV.

The grand potential for PNJL theory in the mean-field approximation is given by the following equation<sup>16</sup>

$$\Omega(\Phi, \bar{\Phi}, m, T, \mu) = \mathcal{U}(\Phi, \bar{\Phi}; T) + G(\bar{q}q)^2 + \Omega_q \quad (7)$$

with (in analogy with (2))

$$\Omega_q = -2N_c N_f \int \frac{d^3p}{(2\pi)^3} E_p - 2N_f T \int \frac{d^3p}{(2\pi)^3} [\ln N_{\Phi}^+(E_p) + \ln N_{\Phi}^-(E_p)]$$

where  $E_p$  is the quark energy,  $E_p = \sqrt{\mathbf{p}^2 + m^2}$ ,  $E_p^{\pm} = E_p \mp \mu$ , and

$$N^+(E_p) = \left[ 1 + 3 \left( \Phi + \bar{\Phi} e^{-\beta E_p^+} \right) e^{-\beta E_p^+} + e^{-3\beta E_p^+} \right], \quad (8)$$

$$N^-(E_p) = \left[ 1 + 3 \left( \bar{\Phi} + \Phi e^{-\beta E_p^-} \right) e^{-\beta E_p^-} + e^{-3\beta E_p^-} \right]. \quad (9)$$

Since the NJL-like models are nonrenormalizable it is needed to introduce a cutoff  $\Lambda$  in momentum integration. Following<sup>16</sup> in this study we use the three dimensional momentum cutoff for vacuum terms and extend this integration till infinity for finite temperatures. A comprehensive study of the differences between the two regularization procedures (with and without cutoff on the quark momentum states at finite temperature) was made in<sup>20</sup>

## 2. Quarks and light mesons in NJL and PNJL models

In the mean-field approximation we can obtain by varying Lagrangians Eq.(1), or Eq.(4) that the constituent quark mass  $m$  is described by the gap equation <sup>14,16</sup>,

$$m = m_0 - 2G \langle \bar{q}q \rangle \quad (10)$$

The quark condensate  $\langle \bar{q}q \rangle$  can be defined by minimizing the thermodynamic potentials Eqs.(2), (7) with respect to the quark mass as  $\partial\Omega/\partial m = 0$ . For the mass equation of both models we get

$$m = m_0 + 8GN_c N_f \int_{\Lambda} \frac{d^3p}{(2\pi)^3} \frac{m}{E_p} [1 - f^+ - f^-], \quad (11)$$

with

$$f^+ = (1 + e^{\beta E_p^+})^{-1}, \quad (12)$$

$$f^- = (1 + e^{\beta E_p^-})^{-1} \quad (13)$$

for the NJL model, and

$$f^+ = \left[ \left( \Phi + 2\bar{\Phi} e^{-\beta E_p^+} \right) e^{-\beta E_p^+} + e^{-3\beta E_p^+} \right] \cdot N_{\Phi}^+(E_p)^{-1}, \quad (14)$$

$$f^- = \left[ \left( \bar{\Phi} + 2\Phi e^{-\beta E_p^-} \right) e^{-\beta E_p^-} + e^{-3\beta E_p^-} \right] \cdot N_{\bar{\Phi}}^-(E_p)^{-1} \quad (15)$$

for the PNJL model, where  $E_p^{\pm} = E_p \mp \mu$ . Moreover, for PNJL calculations we should minimize  $\Omega$  with respect  $\Phi$  and  $\bar{\Phi}$  <sup>16</sup>. One should note, that if  $\Phi \rightarrow 1$ , the expressions Eqs.(14),(15) are reduced to that of the standard NJL model Eqs.(12),(13).

For self-consistent description of the particle spectrum in the mean-field approximation the meson correlations have to be taken into consideration. These correlations are related with the polarization operator of constituent fields. For scalar and pseudoscalar particles the polarization operators are represented by loop-integrals <sup>4,17,18</sup>.

$$\Pi_{ab}^{PP}(P^2) = \int \frac{d^4p}{(2\pi)^4} \text{Tr} [i\gamma_5 \tau^a S(p+P) i\gamma_5 \tau^b S(p)], \quad (16)$$

$$\Pi_{ab}^{SS}(P^2) = \int \frac{d^4p}{(2\pi)^4} \text{Tr} [S(p+P)S(p)], \quad (17)$$

where the operation Tr is taken over both discrete and continuous indexes of quark fields.

From point of view of the polarization operators, the pion and pseudoscalar meson masses can be defined by equations

$$\pi : 1 + 8GN_c N_f \int \frac{d^3p}{(2\pi)^3} \frac{E_p}{P_0^2 - 4E_p^2} (1 - f^+ - f^-) = 0, \quad (18)$$

$$\sigma : 1 + 8GN_c N_f \int \frac{d^3p}{(2\pi)^3} \frac{1}{E_p} \frac{E_p^2 - m^2}{P_0^2 - 4E_p^2} (1 - f^+ - f^-) = 0. \quad (19)$$

Eqs. (10), (18), (19) are solved for model parameters: the cut-off parameter  $\Lambda$ , the current quark mass  $m_0$  (in chiral limit  $m_0 = 0$ ) and the coupling constant  $G$ . These parameters are fixed at  $T = 0$  to reproduce physical quantities: the pion mass  $M_\pi = 0.139$  GeV, the pion decay constant  $F_\pi = 0.092$  GeV and the quark condensate  $\langle \bar{q}q \rangle^{1/3} = -250$  MeV. The obtained parameters are shown in Table 2.

Table 2. The model parameters used for different physics quantities.

$m_0$ [MeV]	$\Lambda$ [GeV]	$G$ [GeV] <sup>-2</sup>	$F_\pi$ [GeV]	$M_\pi$ [GeV]
5.5	0.639	5.227	0.092	0.139

Solutions of the gap-equation Eq.(10) and Eqs. (18), (19) at nonzero  $T$  are presented in Fig. (1). The temperature in the left panel is normalized to the Mott temperature, which defined from condition  $M_\pi = 2m_q$ . In the PNJL model  $T_{\text{Mott}} = 0.27$  GeV and in the NJL model  $T_{\text{Mott}} = 0.208$  GeV for our parameters. Modification

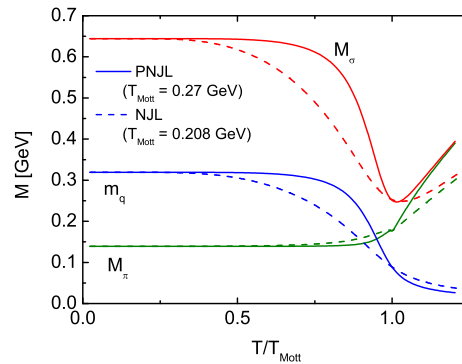


Fig. 1. Temperature dependence of masses  $m_q$ ,  $M_\pi$  and  $M_\sigma$  at  $\mu = 0$  GeV. Results for PNJL and NJL models are given by the solid and dashed lines, respectively.

of quasiparticle properties is clearly seen. The  $\sigma$  mass goes down near the Mott temperature  $T_{\text{Mott}}$  and this fall is sharper in the PNJL model. At  $T/T_{\text{Mott}} > 1$  masses of chiral partners become equal to each other,  $M_\sigma \approx M_\pi$ , and then both masses increase with temperature while the pion mass remains practically constant at  $T/T_{\text{Mott}} < 1$ . The quark mass  $m_q$  also goes down with  $T$  and continues to decrease for temperatures above  $T_{\text{Mott}}$ .

### 3. Thermodynamics of NJL and PNJL models

In order to address the finite density case, it turns out to be useful to introduce for the NJL (or PNJL) model the following effective Lagrangian:

$$\mathcal{L}'_{\text{NJL}} = \mathcal{L}_{\text{NJL}} + \mu \bar{q} \gamma^0 q, \quad (20)$$

which leads to customary grand canonical Hamiltonian. Here the chemical potential  $\mu$  term accounts for baryon number conservation. Thus thermodynamics of particles is described in terms of the grand canonical ensemble which is related with the Hamiltonian  $H$  as follows:

$$e^{-\beta V \Omega} = \text{Tr} e^{-\beta(H - \mu N)}, \quad (21)$$

where  $N$  is the particle number operator and the operator  $\text{Tr}$  is taken over color, flavor and Dirac indices. If  $\Omega$  is known, the basic thermodynamic quantities - the pressure, the energy and entropy densities, the density of quarks number and heat conductivity - can be defined as follows:

$$p = -\frac{\Omega}{V}, \quad (22)$$

$$s = -\left(\frac{\partial \Omega}{\partial T}\right)_{\mu}, \quad (23)$$

$$\varepsilon = -p + T s + \mu n, \quad (24)$$

$$n = -\left(\frac{\partial \Omega}{\partial \mu}\right)_T, \quad (25)$$

$$c = \frac{T}{V} \left(\frac{\partial s}{\partial T}\right)_{\mu}. \quad (26)$$

The thermodynamic potential in the phase transition point has a minimum

$$\frac{\partial \Omega(T, \mu, m)}{\partial m} = 0, \quad \frac{\partial^2 \Omega(T, \mu, m)}{\partial m^2} \geq 0. \quad (27)$$

All these relations describe thermodynamics of the system. In considered models the thermodynamic potentials are defined from Eqs.(2), (7), and from these equations we can get the vacuum part:

$$\Omega_{vac} = \frac{(m - m_0)^2}{4G} - 2N_c N_f \int \frac{d^3 p}{(2\pi)^3} E_p. \quad (28)$$

This quantity does not vanish at  $T \rightarrow 0$  and  $\mu \rightarrow 0$ ; therefore, it is more convenient to use the normalized reduced pressure:

$$\frac{p}{T^4} = \frac{p(T, \mu, m) - p(0, 0, m)}{T^4}. \quad (29)$$

Within the PNJL model with  $\Lambda \rightarrow \infty$  the reduced pressure and energy density exhibit reasonable behavior consistent with the recent lattice QCD results for the vanishing chemical potential<sup>25</sup> (see Fig. 2) keeping in mind that the  $m_{PS}/m_V$  ratio

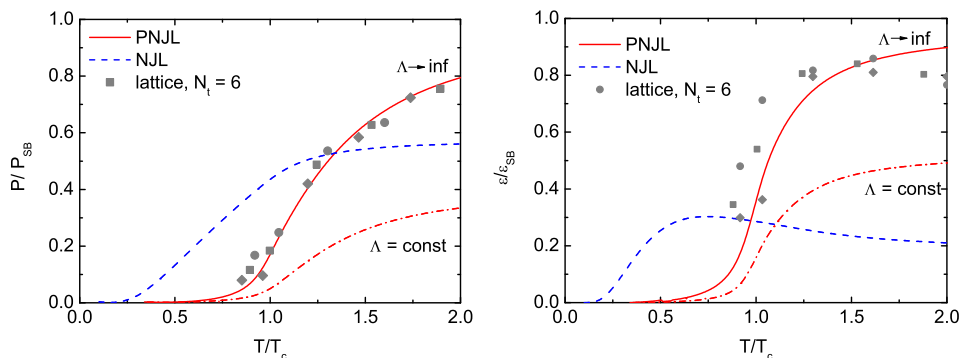


Fig. 2. The temperature dependence of the reduced pressure and energy density within the PNJL model for  $\mu = 0$  in two schemes of regularization  $\Lambda = 0.639$  and  $\Lambda \rightarrow \infty$ . Dotted lines are appropriate results for the NJL model. Lattice data points for  $N_f = 2$  at  $\mu = 0$  are from <sup>23</sup>. Circles, squares and diamonds correspond to calculations at  $N_t = 6$  with the mass ratio of the pseudoscalar to vector meson  $m_{PS}/m_V = 0.65, 0.70$  and  $0.75$ , respectively.

in lattice calculations is still far from that for physical masses  $m_{PS}/m_V \sim 0.2$ . One should note that both models have the cut-off parameter  $\Lambda$  <sup>16</sup>. But the integrals containing logarithm both in Eq.(2) and Eq.(7) are convergent <sup>10,23</sup>. In our work we calculated these integrals with  $\Lambda \rightarrow \infty$ . It leads to the flattening of pressure at high temperature. However most integrals for PNJL model are convergent too. It was the reason to consider the thermodynamic functions behavior at  $\Lambda \rightarrow \infty$ . It was supposed that with increasing temperature the pressure have to reach the Stefan-Boltzmann limit <sup>20</sup>, which in PNJL model is defined as

$$\frac{p_{SB}}{T^4} = (N_c^2 - 1) \frac{\pi^2}{45} + N_c N_f \frac{7\pi^2}{180} \simeq 4.053. \quad (30)$$

If the regularization  $\Lambda = 0.639$  is used, the  $T$ -shape of the thermodynamic quantities considered is roughly the same while their absolute values are noticeably lower, being far from the Stefan-Boltzmann limit. In the NJL model the  $p/T^4$ , and  $\epsilon/T^4$  are not only underestimated but also essentially shifted toward lower temperatures.

Within NJL-like models there are several characteristic temperatures. The parameter  $T_0$  entering the effective potential (6) of the PNJL model has been noted above. Three other scales are the pseudo-transition temperature for chiral crossover  $T_\chi$  defined by the maximum of  $\partial\langle q\bar{q}\rangle/\partial T$ , the pseudo-transition temperature for deconfinement crossover  $T_p$  which can be found from the maximum of  $\partial\Phi/\partial T$ , and  $T_c$  defined for PNJL model as the average of two transition temperatures  $T_\chi$  and  $T_p$  <sup>10,15</sup>. The temperature dependence of the order parameters for the chiral  $\langle q\bar{q}\rangle$  and deconfinement  $\Phi$  phase transitions, are shown in Fig. (3). The chiral condensate decreases and the Polyakov loop potential increases with  $T$ , demonstrating closeness of  $T_\chi$  and  $T_p$  temperatures at  $\mu = 0$  (see also Table 3). For  $\pi$ -mesons, the Mott temperature  $T_{\text{Mott}}$  is provided by the condition  $M_\pi = 2m_q$  and similarly  $\sigma$ -meson

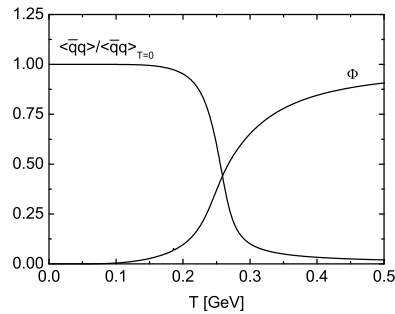


Fig. 3. Temperature dependence of the chiral condensate and Polyakov loop potential at  $\mu = 0$  GeV within the PNJL model

dissociation temperature  $T_d^\sigma$  is given by the equation  $M_\sigma = 2M_\pi$ <sup>18,19</sup>. All these quantities obtained at  $\mu = 0$  are presented in Table 3.

Table 3. Characteristic temperatures in NJL and PNJL models.

	$T_0$	$T_\chi$	$T_p$	$T_c$	$T_{\text{Mott}}$	$T_d^\sigma$
NJL	–	0.192	–	0.192	0.207	0.185
PNJL	0.27	0.249	0.258	0.253	0.27	0.259

Phase diagrams in  $(T - \mu)$  plane for nonzero chemical potential  $\mu$  are given in Fig.4. As is seen the chiral transition line, determined by<sup>4</sup>

$$\left[ \frac{1}{4G} + \frac{\partial \Omega_q}{\partial m^2} \right]_{m=0} = 0$$

in both NJL and PNJL models, is a monotonously decreasing function of the chemical potential. In the limiting chirally symmetric case corresponding to  $m = 0$  the  $T_\chi$  at large  $\mu$  is higher than those for finite mass but both temperatures coincide when  $\mu \rightarrow 0$  as for the NJL and PNJL models. For the case  $\mu \neq 0$  both models show the critical end point at the temperature  $T_{CEP}$  below which the chiral phase transition is of the first order. At this point  $(T_{CEP}, \mu_{CEP})$  a phase transition becomes the second order but for the temperature higher than  $T_\chi$  we meet a crossover<sup>20,21,22</sup>. For chiral symmetric case in the PNJL model the first order phase transition ends at a tricritical above which,  $T > T_{TCP}$ , the chiral transition is of the second order while in the NJL model<sup>26</sup> the transition is of the first order everywhere besides the tricritical point at  $\mu = 0$  where it is of the second one. In accordance with other calculations, the temperature of tricritical transition is above that of the critical end point. Within the PNJL model the positions of critical points are  $(T_{CEP}, \mu_{CEP}) = (95, 320)$  and  $(T_{TCP}, \mu_{TCP}) = (160, 265)$  MeV. These numbers are quite close to those in<sup>20</sup> for the similar parameter set (set B, the case I). One



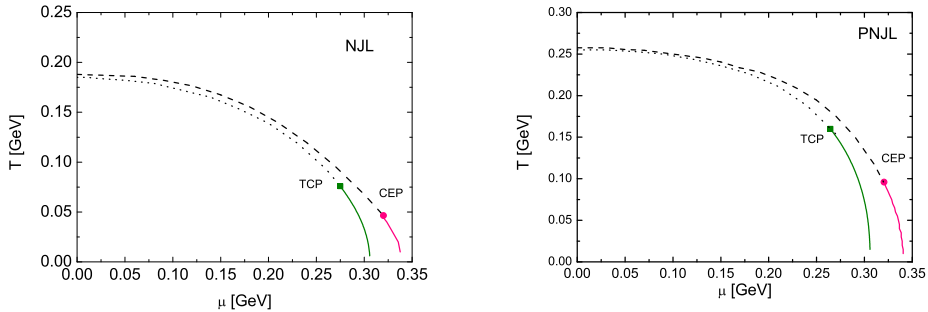


Fig. 4. Phase diagrams of NJL (left panel) and PNJL (right panel) models. Solid lines correspond to the first order phase transition, dashed lines are crossover and dotted lines are the boundary of the second order phase transition.

should emphasize that critical properties of observables are significantly influenced by the chosen parameter set and regularization procedure as was demonstrated in 20.

#### 4. Conclusion

We compare the constructed NJL and PNJL models. In agreement with previous results, it is shown that the inclusion of coupling between chiral symmetry and deconfinement essentially improves the description of thermodynamic bulk properties of a medium. The models qualitatively reproduce both meson properties in such environment and its rich and complicated phase structure. Effects of the Polyakov loop move the CEP to higher  $T$  and lower  $\mu$  than the NJL predicts<sup>15</sup>. The position of the calculated CEP in the  $(T - \mu)$  plane is still far from the predictions of lattice QCD and empirical analysis and more elaborated models are needed.

#### Acknowledgments

We are grateful to P. Costa and V.V. Skokov for useful comments. V.T acknowledges a financial support within the “HIC for FAIR” center of the “LOEWE” program. The work of Yu. K. was supported by the RFFI grant 09-01-00770a.

#### References

1. Y. Nambu and G.Jona-Lasinio, Phys. Rev. **122**, 345 (1961).
2. M.K.Volkov, Annals of Physics **157**, 282 (1984).
3. U. Vogel and W. Weise, Progr. Part. Nucl. Phys. **27**, 195 (1991).
4. S.P. Klevansky, Rev. Mod. Phys. **64**, 649 (1992).
5. T. Hatsuda and T. Kunihiro, Phys. Rep. **27**, 221 (1994).
6. M. Buballa, Phys. Rep. **407**, 205, (2005).
7. M.K.Volkov, A.E. Radzhabov, Phys. Usp. **49**, 551 (2006).
8. P.M. Meisinger, T.R. Miller, and M.C. Ogilvie, Phys. Rev. **D 65**, 034009 (2002).

9. K. Fukushima, Phys. Lett. **B 591**, 277 (2004).
10. C.Ratti, M.A. Thaler and W. Weise, Phys. Rev. **D 73**, 014019 (2006).
11. E. Megias, E. Ruis Ariolla and L.L. Salcedo, Phys. Rev. **D 74**, 065005 (2006).
12. S.K. Ghosh, T.K. Mukherji, M.G. Mustafa and R. Ray, Phys. Rev. **D 73**, 114007 (2006)
13. M. Asakava and K. Yasaki, Nucl. Phys. **A504**, 668 (1989).
14. J.Hüfner, S.P. Klevansky and P. Zhuang, Acta Phys. Pol. **B 25**, 85 (1994).
15. S.Rössner, C. Ratti and W.Weise, Phys.Rev. **D 75**, 034007 (2007)
16. H. Hansen, W.M.Flberico, A. Beraudo, A. Molinari, M. Nardi and C. Ratti, Phys. Rev. **D 75**, 065004 (2007).
17. H.J. Schulze, J. Phys. **G 21**, 185 (1995).
18. E. Quack, P. Zhuang, Y. Kalinovsky, S.P. Klevansky and J. Hüfner, Phys.Lett, **B348**,1, (1995).
19. W.J. Fu and Y.X. Liu Phys. Rev. **D 79**, 074011, (2009).
20. P. Costa, M.C. Ruivo, H. Hansen and C.A. de Sousa, Phys. Rev. **D 81**, 016007, (2010); hep-ph/0909.5124.
21. K. Kashiwa, H. Kuono. M. Matsuzaki and M. Yahiro, Phys. Lett. **B 662**, 26, (2008).
22. K. Fukushima, Phys. Rev. **D 78**, 114019 (2008).
23. C.Sasaki, B. Friman and K. Redlich, Phys. Rev. **D 75**, 054026 (2007).
24. Z. Zhang and Y.X. Liu, Phys. Rev. **C 75**, 064910 (2007)
25. A. Ali Khan at al., Phys. Rev. **D64**, 074510 (2001).
26. O. Scavenius, A. Mocsy, I.N. Mishustin and D.H. Rischke, Phys. Rev. **C64**, 045202 (2001).